Chapter 4

The Impact of the Use of Large Non-Linear Lighting Loads in Low-Voltage Networks

Natalio Milardovich, Leandro Prevosto, Miguel A. Lara and Diego Milardovich

Additional information is available at the end of the chapter

http://dx.doi.org/10.5772/intechopen.76752

Abstract

The principal numerical and experimental results obtained by the authors on the harmonic power losses in low-voltage networks in the lighting area have been summarized in this review. Light-emitting diodes (LEDs) and compact fluorescent lamp (CFL) loads were considered. Four-core cables and four single-core cable arrangements were examined. The cables were modeled by using electromagnetic finite element analysis software. It was found that the cross section of the neutral conductor plays an important role in the derating of the cable ampacity due to the presence of a high level of triplen harmonics in the distorted current. In order to reduce the third-order harmonic currents in the neutral conductor, an experimental investigation of diversity factors for LED in combination with CFL and LED lamps was also performed. Attention was paid to the reduction of the third-order harmonic current, which is mainly responsible for the strong increase in power losses in the neutral conductor of low-voltage installations. The convenience of having LED lamps designed to operate as two-phase loads is suggested for certain applications.

Keywords: LED, CFL, non-linear lighting loads, harmonic currents, energy losses, low-voltage networks

1. Introduction

Today, non-linear devices constitute a bigger part of the electrical load in industrial and commercial power systems. Non-linear devices generate harmonics in line currents, resulting in a large number of problems for electrical equipment, such as capacitors, circuit breakers, electronic equipment, metering, conductors and telephones [1–3]. The presence of harmonic currents in electric systems has increased in recent times due to several factors (increased use

of solid-state energy conversion devices, industrial variable speed drive systems and cutting and welding equipment). Significant sources of harmonic currents in power systems also include electric devices such as compact fluorescent lamps (CFLs), power transformers operating near saturation and computer system installations [4–6].

Nowadays, with the technological advancement in semiconductors, light-emitting diode (LED) lamps are becoming a promising lighting technology due to its superior energy efficiency, longer lifetime and a better visual performance compared to most of the conventional light sources [7–9]. Due to these unique features, CFLs are now being replaced by LED, seeking a reduction in lighting costs and a lower impact on environment. In general lighting applications, a compact ac/dc (alternating current/direct current) converter should be used to supply dc current to LEDs, which introduces non-linearity to the system [10–12]. As non-linear loads, LEDs might produce highly distorted currents. Although the input power of a single LED is quite low, an incoming widespread use of them in lighting could create significant additional harmonic losses in the existing low-voltage lines [13]. Since several national standards allow for the neutral conductor reducing sizing with respect to the phase conductors, many of these existing low-voltage installations have the cross section of the neutral conductor approximately equal to half of the phase conductors.

A large number of works were conducted on LEDs as an energy-efficient lamp, but most of them have been devoted to the internal driver circuit design [10–12, 14–17]. Several other works have concentrated on the light distribution and visual performance of LED lamps [18–20]. A few contributions focused on harmonic emissions of LED lamps [12, 21–24].

When significant harmonic currents are present in low-voltage supply systems, additional Joule losses occur in the phase or line conductors as well as the neutral conductor. Significant harmonic currents may be present in secondary circuits of three-phase wye-connected transformers and single-phase transformers. Zero sequence harmonic currents flow in the phase conductors and are added in the neutral conductor, thus resulting in even higher harmonic current flow in the neutral conductor [25, 26]. Thus, the harmonic current flow in the neutral must be considered in the design of the supply system. The presence of harmonic currents in the supply conductors affects the ampacity of the supply system because of the additional ohmic losses [13, 26–28]. The determination of ohmic losses is complicated by the fact that the resistance of the cables is frequency dependent. Specifically, the resistance is increased with frequency because of the skin effect and proximity effect in the conductors and proximity effect from metallic conduit (if present) [26, 29]. The effects of harmonic currents in the neutral conductors can be evaluated with the same methods as for the phase or line conductors. However, the harmonic current magnitudes may be different in the neutral conductors due to non-cancelation of zero sequence harmonic currents and the cancelation of the positive and negative sequence harmonic currents. Thus, the neutral conductor becomes an additional heat-generating conductor and must be considered in the ampacity calculation for three-phase wye-connected and single-phase circuits [26–28]. Besides the knowledge of the increased losses due to harmonic currents, it is significant also for the economic evaluation of measures that attenuate harmonic currents. Such measures can be, for instance, passive or active harmonic filters [30, 31] or controlling the current unbalance in three-phase distribution systems by node reconfiguration [32].

A research on the diversity factor for combinations of LED lamps with powers in the range 3 to 8 W was presented in [33]. It was found that the diversity factor becomes smaller if a large number of lamps are combined. However, such a reduction was more significant for high-order harmonic currents. In particular, a diversity factor close to one for the third-order harmonic was found for the combinations studied. In [34] an investigation was presented on the diversity factor for combinations of LED and FCL lamps. The measurements showed a considerable reduction of the diversity factor for higher harmonic currents, but, on the other hand, the low-order harmonics did not show a significant decrease.

The principal numerical and experimental results obtained by the authors on the harmonic power losses in low-voltage networks feeding large LED and CFL loads have been summarized in this review. Attention was paid to the reduction of low-order harmonic currents, especially the third one, which is mainly responsible for the strong increase in power losses in the neutral conductor of low-voltage installations [13]. The convenience of having LED lamps designed to operate as two-phase loads is suggested for certain applications of significant power demand.

2. Harmonic losses in low-voltage networks

2.1. Harmonic emission of LED and CFL

Figure 1 shows the current in one phase and in the neutral conductor of a four-core cable that feeds a balanced load of three identical LEDs (one per phase). Specifically, **Figure 1** was obtained by testing the Philips 8 W LED. It can be seen that the LED current is highly distorted with respect to a sinusoidal waveform and that the fundamental frequency of the current in the neutral conductor is 150 Hz (i.e. the frequency of the third harmonic). Because the third-order harmonic currents (and their multiples) are zero sequence, they are added to the neutral

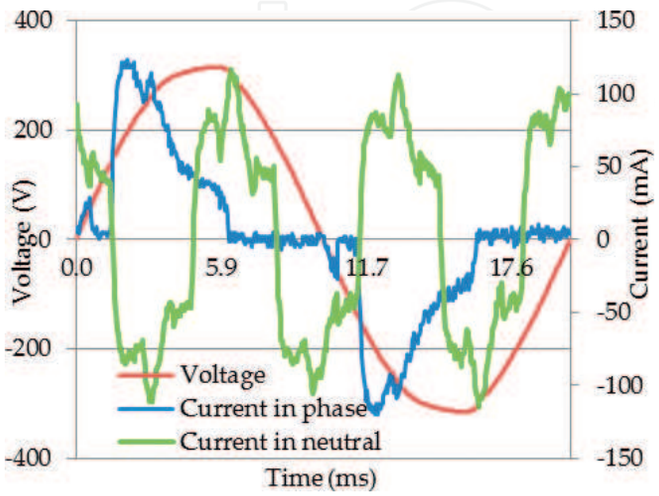

Figure 1. Voltage and current waveforms in one phase and current in the neutral conductor [35].

conductor. All experiments were done with an almost sinusoidal voltage waveform. The total harmonic distortion (THD) of the phase voltage waveform was relatively low (< 3%).

A frequency domain analysis of the current harmonics ($I_{pu}(h)$) produced by several commercially available LEDs is presented in **Figure 2**. In this figure, $I_{pu}(h)$ was expressed in per unit of the fundamental current harmonic ($h = 1$ corresponding to a harmonic frequency of $f = 50$ Hz, with h being the order of the harmonic).

The experimental data can be approximately described by the power law:

$$\frac{I(h)}{I(1)} = h^m, \tag{1}$$

where $m = -1.2 \pm 0.2$. Eq. (1) (which is indicated by a solid line in **Figure 2**) defines the harmonic signature of the examined LED lamps. It is observed in **Figure 2** that the amplitude of the harmonic currents decreases almost inversely with the order of the harmonic, thus indicating that the third-order one is usually the most significant one. Note that the data corresponded to LEDs from 3 to 120 W. FCLs also tend to present considerable amplitudes in their third-order harmonics [34]. **Figure 3** shows the amplitude of the third harmonic current (expressed in per unit of the fundamental harmonic) of several commercially available LEDs and CFLs, with powers varying between 3 and 23 W. The red line (representing a constant value of 86%) indicates one of the criteria established by IEC 61000–3-2 [36] for the harmonic emission limits for lamps having an active input power < 25 W (i.e. that the third harmonic current should not exceed 86% of the fundamental one).

As it can be seen in **Figure 3**, the lamps tested meet the quoted emission limit imposed by IEC, except for one of them (LED 9 W Sica), which is slightly above it.

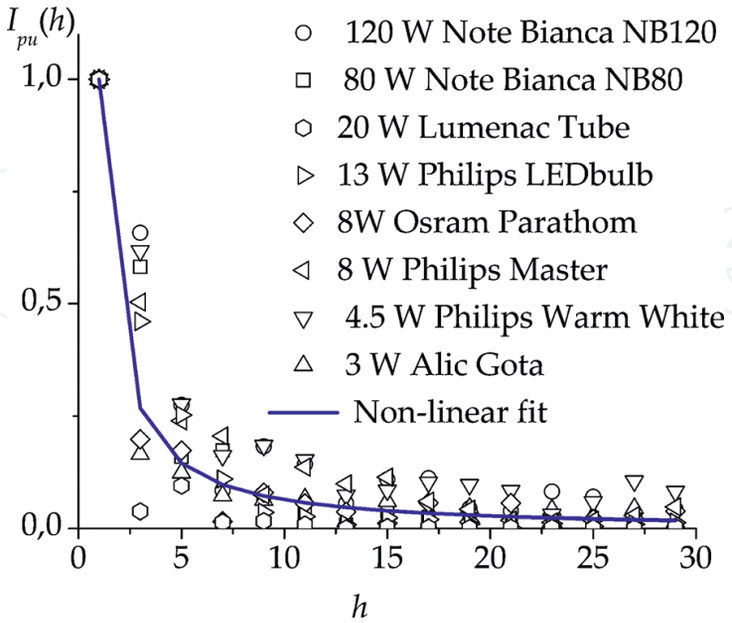

Figure 2. Frequency domain analysis of the current harmonics on several commercially available LEDs. The blue line represents the power law given by Eq. (1) [13].

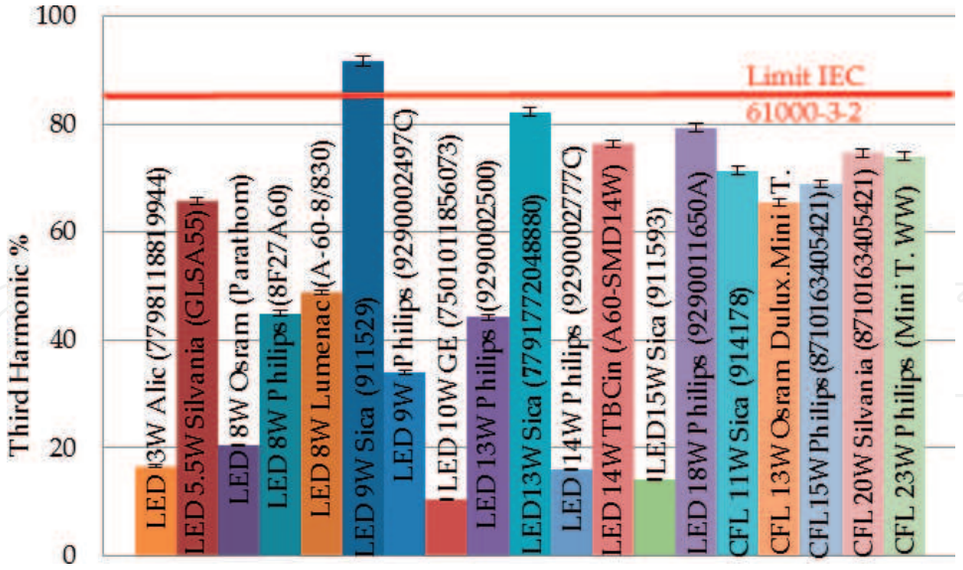

Figure 3. Third-order harmonic current amplitude for the investigated lamps [35].

A power quality analyzer (Fluke 435-II) was used in the measurements presented here.

2.2. Numerical simulation of the harmonic losses in low-voltage networks

Two different types of cables were examined. The first type was an arrangement of four single-core cables in contact with each other, as they are specified by IEC 60502–1 [37]. The schematic of the used cable arrangement is shown in **Figure 4**, while its geometric dimensions are summarized in **Table 1**.

As the conductors in all cables were assumed solid in the modeling, the conductor dimensions showed in **Table 1** are slightly smaller than the actual dimensions. This assumption leads to results that are on the conservative side. Cases where the conductors were copper and the cross section of the neutral conductor was approximately equal to half of phase conductors were modeled.

The second type corresponded to four-core cables as they were specified by CENELEC Standard HD603 [38]. In this case, a large cross-sectional sector-shaped cable, namely, $3 \times 240 + 120$ mm^2, was examined.

In a conductor where the conductivity is sufficiently high, the displacement current density can be neglected, and the conduction current density is given by the product of the electric field and the electrical conductivity (ohm's law). With these simplifications, the Maxwell's equations are

$$\nabla \times \left(\frac{\overline{B}}{\mu}\right) = \sigma \overline{E}, \tag{2}$$

$$\nabla \times \overline{E} = -\frac{\partial \overline{B}}{\partial t}, \tag{3}$$

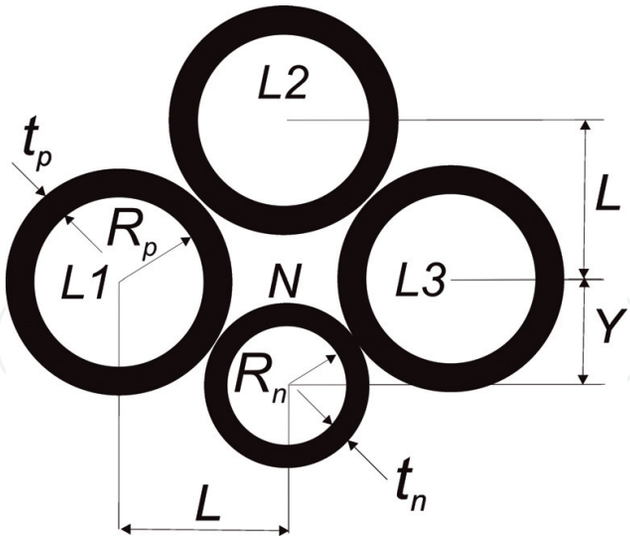

Figure 4. Layout of the examined single-core arrangement (taken from [13]).

	Nominal cable cross section [mm^2]			
Dimensions [mm]	3 × 35 + 16	3 × 70 + 35	3 × 120 + 70	3 × 240 + 120
Phase conductor radius [R_p]	3.3	4.7	6.2	8.8
Neutral conductor radius [R_n]	2.3	3.3	4.7	6.2
Thickness of phase conductor insulation [t_p]	2.6	2.8	3.1	4.0
Thickness of neutral conductor insulation [t_n]	2.4	2.6	2.8	3.1
Distance [L]	8.4	10.6	13.1	18.0
Distance [Y]	6.5	8.2	10.5	12.7

Table 1. Dimensions of the modeled cable arrangement.

where $\overline{B}$ is the magnetic field, μ is the magnetic permeability, σ is the conductor electrical conductivity and $\overline{E}$ is the electric field. Introducing the magnetic vector potential $\overline{A}$ ($\overline{B} \equiv \nabla \times \overline{A}$) in Eq. (3), $\overline{E}$ can be expressed as

$$\overline{E} = -\nabla V - \frac{\partial \overline{A}}{\partial t}, \tag{4}$$

(where V is the electrostatic potential), and Eq. (2) becomes

$$\nabla \times \left[\frac{\nabla \times \overline{A}}{\mu}\right] = -\sigma \nabla V - \sigma \frac{\partial \overline{A}}{\partial t}. \tag{5}$$

The electromagnetic software [39] solved the diffusion equation (Eq. (5)) to obtain the spatial distribution of the total current density ($\bar{J}$) over each conductor's surface (S), having as input the measurable current in the conductor:

$$\begin{aligned} I &= \int \bar{J} \cdot d\bar{S} = \int \left(\bar{J}_0 + \bar{J}_{eddy}\right) \cdot d\bar{S} \\ &= \frac{V}{R_{dc}} - \sigma \int \frac{\partial \bar{A}}{\partial t} \cdot d\bar{S}, \end{aligned} \tag{6}$$

where I is the total current and R_{dc} is the dc conductor resistance ($\bar{J}_0$ is the spatial average current density generated by potential electric fields, while $\bar{J}_{eddy}$ is the (eddy) current density induced by rotational fields). Eq. (6) assumed a uniform electrical conductivity over the conductor surface. This is justified because simple estimates showed that the temperature variations over the conductor's surface

$$\Delta T \approx \frac{\Lambda^2}{\kappa} \sigma E^2, \tag{7}$$

(where κ is the conductor thermal conductivity and $\Lambda = R/2.4$ and R is the conductor radius) due to the non-uniform distribution of the Joule heat caused by the skin and proximity effects are very small because of the large value of the thermal conductivity.

At each harmonic frequency, the software calculates the losses per unit length in each conductor using the integral:

$$P(h) = \frac{1}{\sigma} \int J(h)^2 \, dS, \tag{8}$$

where $P(h)$ is the harmonic losses per unit conductor length and $J(h)$ is the current density corresponding to the harmonic of order h.

The cables were modeled in two dimensions assuming that at each harmonic frequency, balanced, three-phase and sinusoidal currents flow through them. The three-phase conductors were assumed carrying the following currents:

$$I_{L1} = I_p \cos\left(2\pi h f t + \phi_h\right), \tag{9}$$

$$I_{L2} = I_p \cos\left(2\pi h f t - h \frac{2}{3}\pi + \phi_h\right), \tag{10}$$

$$I_{L3} = I_p \cos\left(2\pi h f t + h \frac{2}{3}\pi + \phi_h\right), \tag{11}$$

where I_p is the current peak value, φ_h is the angle phase of the harmonic order h and $L1$, $L2$ and $L3$ are the three phases.

For non-triplen harmonic ($h \neq 3\,N$, with $N = 1, 2, 3, \ldots$), the neutral conductor only carries the eddy currents calculated by the software. Notice that in this case, $h = 3\,N + 1$ represents the direct sequence harmonics, while $h = 3\,N - 1$ represents inverse sequence harmonics. For triplen harmonics the current in the neutral conductor was assumed as

$$I_N = 3I_p \cos(2\pi hft + \pi). \tag{12}$$

In order to obtain an accurate distribution of the current density over the conductor sections, it was checked that the size of the local numerical mesh was less than half the characteristic skin penetration length for each harmonic order.

The study domain for the cases of sector-shaped and four single-core cables, showing the non-uniform numerical grid (with up to about 4000 mesh cells), is presented in **Figure 5**. At the boundary of the domain (at a radius up to ten times the cable size), it was assumed that $\overline{A} = 0$ because the magnetic field vanishes at a large distance (as compared to the cable size) from the cable.

The simulation results were obtained for $\mu = 4\ \pi \times 10^{-7}$ H/m (non-magnetic material was considered). The copper electrical conductivity at 293 K was taken as $\sigma = 5.8 \times 10^7\ \Omega^{-1}\ m^{-1}$ according to IEC 60028 [40]. The σ value was correspondingly corrected for other cable operating temperatures.

Figure 6 illustrates the spatial distribution of the root-mean-square (rms) value of the total current density over the conductors of cables of large sections submitted to harmonic currents of different frequencies. **Figure 6(a)** corresponds to a $3 \times 240 + 120$ mm^2 sector-shaped cable submitted to a 15 A (peak value) fifth-order harmonic current, while **Figure 6(b)** corresponds to an arrangement of four single-core cables ($3 \times 70 + 35$ mm^2) submitted to a 30 A (peak value) third-order harmonic current. The magnetic field lines produced by the current are also shown in **Figure 6**. A noticeable reduction in the effective area of current circulation due to the skin and proximity effects is observed in **Figure 6(a)**, thus causing a considerable increase of the ac conductor resistance (Rac) as compared to the dc resistance, (Rdc), which in turn results in high heat losses. In **Figure 6(b)** the neutral conductor is assumed to carry the algebraic sum of the phase currents.

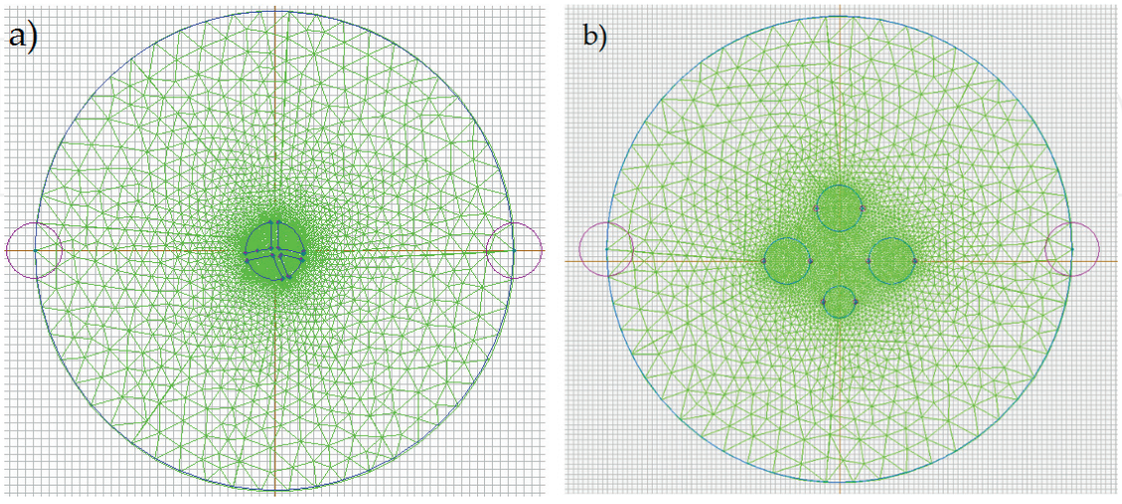

Figure 5. Non-uniform numerical grid generated by the software for the case of a four-core sector-shaped cable (a) and four single-core cables (b).

http://dx.doi.org/10.5772/intechopen.76752

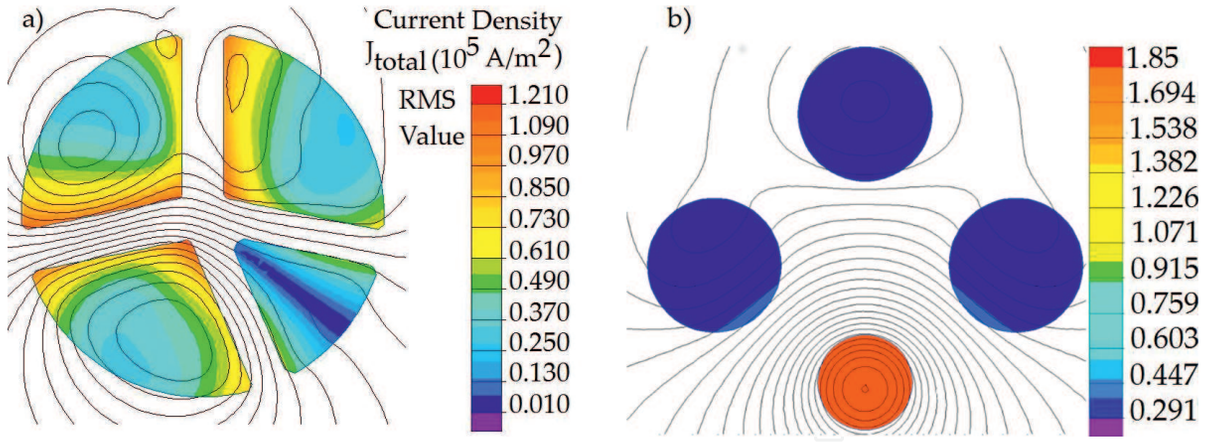

Figure 6. Spatial distribution of the rms current density for the fifth-order (h = 5) harmonic in a sector-shaped cable of 3 × 240 + 120 mm^2 (a) and for the third-order (h = 3) harmonic in four single-core cables of 3 × 70 + 35 mm^2 (b).

To calculate the R_{ac} conductor resistance, an ac steady-state harmonic analysis was employed. Only the odd harmonics, up to the 29th, were considered. A higher value of this upper limit did not have appreciable impact to the obtained results. Due to the geometry of the cables, the losses in the phase conductors are not identical. In fact, the losses in phase conductors $L1$ and $L3$ (**Figure 4**) are the same, but those in $L2$ are different. The losses per unit length in the three-phase conductors, when a symmetrical current of rms value $I_{rms}(h)$ and of frequency $f\,h$ flows through them, can be defined as $P_{L1}(h)$, $P_{L2}(h)$ and $P_{L3}(h)$, for $L1$, L2 and $L3$, respectively. The uneven heat generation inside the cable is a fact that also needs to be considered when calculating the derating of cable ampacity. According to [41], not only the average cable temperature but also the temperature at any point along the insulation of the cable should not exceed the maximum permissible one. Therefore, for derating of the cable ampacity, the maximum conductor losses should be considered and not their average. For non-triplen harmonic ($h \neq 3\ N$), the neutral conductor only carries the eddy currents calculated by the software, so the maximum cable losses can be represented by an effective conductor resistance per unit length $R_{eff}(h)$ for the harmonic order h, which was defined as

$$3P_{L\max}(h) \;+\; P_N(h) \;\equiv\; 3{I_{rms}}^2(h)\,R_{eff}(h)\;, \tag{13}$$

where

$$P_{L\,\max}(h) \;\equiv\; \max\{P_{L1}(h), P_{L2}(h), P_{L3}(h)\}. \tag{14}$$

When triplen harmonics are present, the neutral conductor picks up the current. An effective resistance that reflects the maximum losses of the phase conductors ($\tilde{R}_{eff}(h)$) and another resistance ($R_{ac\,N}(h)$) that reflects the losses of the neutral conductor were defined as

$$3P_{L\max}(h) \;\equiv\; 3{I_{rms}}^2(h)\,\tilde{R}_{eff}(h)\;, \tag{15}$$

$$P_N(h) \;\equiv\; {I_{rms\,N}}^2(h)\,R_{ac\,N}(h)\;, \tag{16}$$

where

$$I_{rms\,N}(h) \equiv 3\ I_{rms}(h), \tag{17}$$

is the neutral conductor current for the harmonic current of order h. The resistances $R_{eff}(h)$ and $\tilde{R}_{eff}(h)$ will be referred, from now on, as $R_{ac}(h)$. The ratio $R_{ac}(h)/R_{dc}$ for the phase and neutral conductors of the cables described in **Table 1** and for a $3 \times 240 + 120$ mm^2 four-core cable are shown in **Figures 7(a)** and **(b)**, respectively. As expected, the ratio $R_{ac}(h)/R_{dc}$ for the phase conductors increases with both frequency and conductor cross section due to skin and proximity effects. The curve is not smooth but presents spikes at triplen harmonics.

This is mainly due to the increased losses in conductors $L1$ and $L3$ when zero sequence currents flow in the phase conductors and thereby in the neutral conductors. The ratio $R_{ac}(h)/R_{dc}$ for the neutral conductor is shown only for triplen harmonics, because only when triplen harmonics are present the neutral conductor picks up the current (other than eddy currents). It is evident from **Figures 7(a)** and **(b)** that the ratio of the neutral conductor is much smaller than that of the respective phase conductors. This occurs because the zero sequence currents decrease the proximity effect significantly on the neutral conductor when its position, relative to the phase conductors, is as shown in **Figure 4**.

The simulation results corresponded to a conductor operating temperature of 343 K, which is the maximum conductor temperature for PVC-insulated cables according to IEC 60502–1 [12]. It was checked that large variations in this temperature value (in the range 283 to 343 K) only render slightly variations (less than 10%) in the conductor resistance ratio. The results of the employed electromagnetic model were validated by comparison to (a) the numerical model developed in [27] and (b) the formulae given in the standard IEC 60287–1-1 [42] for thee single-core cable arrangements. The differences in the calculated ratios $R_{ac}(h)/R_{dc}$ were in both cases less than 3% in the whole considered frequency range.

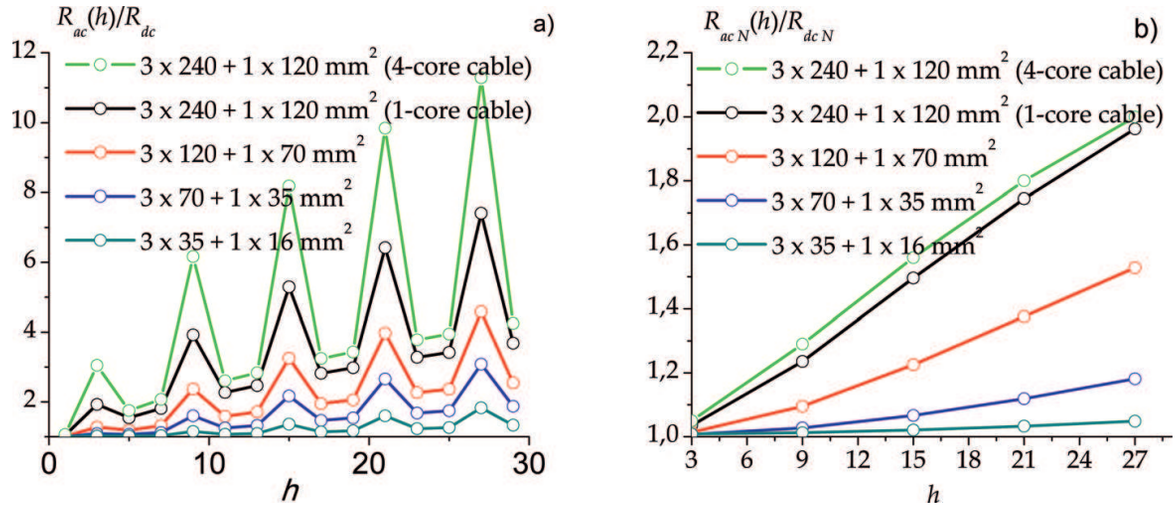

Figure 7. Variation with the harmonic order of the ratio $R_{ac}(h)/R_{dc}$ for various examined cables, (a) for the phase conductors and (b) for the neutral conductor.

The cable losses can be approximately calculated by the following formula:

$$P_{loss} = 3\sum_{h=1}^{29} {I_{rms}}^2(h)\,R_{ac}(h) + \sum_{h=3N}^{27} (3I_{rms}(h))^2 R_{ac\,N}(h), \tag{18}$$

where the first term on the right-hand side represents the losses in the phase conductors and the second term is the losses in the neutral conductor. This second term is present only when triplen harmonics are considered (i.e. $h = 3, 9, 15, 21, 29$). The values of $R_{ac}(h)$ and $R_{ac\,N}(h)$ were shown in **Figures 7(a)** and **(b)**, respectively. It is important to compare the above calculated cable losses (Eq. (18)) with the losses produced in an identical cable but carrying an undistorted electric current of a rms value of $I_{rms}(1)$. To do this, the cable losses ratio defined as

$$\xi \equiv \frac{P_{loss}}{3\,{I_{rms}}^2(1)\,R_{ac}(1)}, \tag{19}$$

were calculated by using the harmonic signature given by Eq. (1) for the cables described in **Table 1** and for a $3 \times 240 + 120$ mm^2 four-core cable as was specified by CENELEC Standard HD603 [38]. The results obtained for the upper bound of m ($= -1.0$) are shown in **Table 2**. The assumption on the m value leads to results that are on the conservative side.

As it is observed in **Table 2**, for a four-core cable with a cross section of 3 x 240 + 120 mm^2, the power losses reach 2.5 times the value corresponding to an undistorted current of the same rms value of the first harmonic of the LED current. Even for cables with relatively small cross sections, such as $3 \times 35 + 16$ mm^2, this ratio reaches about 2.1. Furthermore, if the skin and proximity effects are neglected in the cable losses given by Eq. (18) (the conductor radius is small as compared to the characteristic skin penetration length and the distances of the nearby conductors are large as compared to the conductor radius) and thus ξ is not dependent on the cable cross section, the loss ratio still reaches 2.0 for $m = -1.0$. The increase in the losses is mainly due to the harmonic content of the distorted current.

As shown **Table 2**, large LED-like loads generate huge harmonic losses resulting in additional conductor heating. This heating will result in a higher-temperature rise of the cable which can exceed its rated temperature, thus requiring the derating of the cable ampacity.

Cable type	**Nominal cable cross section [mm^2]**	ξ
Arrangement of four single-core cables	$3 \times 35 + 16$	2.1
	$3 \times 70 + 35$	2.1
	$3 \times 120 + 70$	2.0
	$3 \times 240 + 120$	2.3
Four-core cable	$3 \times 240 + 120$	2.5

Table 2. Calculated cable loss ratio ξ of various examined PVC-insulated low-voltage cables feeding LED-type loads.

3. Reduction of the harmonic losses in low-voltage networks

In order to reduce the third-order harmonic currents by properly combining lamps that have an important phase difference in their corresponding harmonic currents (rather than combining lamps in a random way), the phase angle ($\varphi 3$) of the third-order harmonic currents was first measured (with respect to the fundamental harmonic voltage angle of the phase 1) for the CFL and LED lamps. The results are given in **Table 3**.

Data in **Table 3** correspond to time-averaged values over an interval of 5 minutes with a sampling rate of 1 S/s. The data were taken applying nominal voltage to the lamps once they acquired their stable working temperature. A power quality analyzer (Fluke 435-II) was used in the measurements. The experimental uncertainty (mainly due to statistical fluctuations) was within $\pm 5^{\circ}$. In order to match the measuring range of the instrument used to the relatively small currents of the lamp combinations, the currents were measured by using low-inductance (around 0.1 mH) coils. It was verified during the measurements that the inductance introduced in the circuit by the coils does not appreciably affect the results. The uncertainty ($\pm$ 2%) in the current measurement due to the position sensitivity of the used flexible current probe was accounted for. The information provided by the instrument was processed through the PowerLog 4.3.1 software.

During the measurements, the phase angles of the third-order harmonic currents were remarkably stable as shown in **Figure 8**. The corresponding experimental uncertainty (mainly due to statistical fluctuations) was within $\pm 5^{\circ}$.

In order to achieve a considerable attenuation effect of the third-order harmonic currents for a given combination of lamps, they should not only fulfil with the condition that its third-order harmonic be strongly out of phase (as is the case of LED Alic 3 W and LED Philips 8 W), but also the amplitudes of each harmonic current should be similar, i.e. the ratio between the amplitudes of the third-order harmonic current of each lamp should be approximately united. **Table 4** shows the results of the ratio between the amplitudes of the third-order harmonic

Lamp type	φ_3 (degrees)	Lamp type	φ_3 (degrees)
LED Alic 3 W	95	LED Philips 14 W	−33
LED Sylvania 5.5 W	−112	LED TBC in 14 W	−126
LED Osram 8 W	−126	LED Sica 15 W	−130
LED Philips 8 W	−77	LED Philips 18 W	−125
LED Lumenac 8 W	−9	CFL Sica 11 W	−114
LED Sica 9 W	−153	CFL Osram 13 W	−111
LED Philips 9 W	−9	CFL Philips 15 W	−111
LED GE 10 W	−49	CFL Sylvania 20 W	−119
LED Philips 13 W	2	CFL Philips 23 W	−108
LED Sica 13 W	−129		

Table 3. Angle of the third-order harmonic current of the lamps used [35].

http://dx.doi.org/10.5772/intechopen.76752

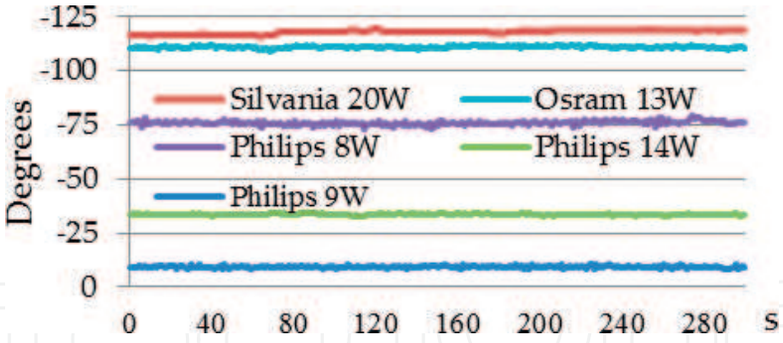

Figure 8. Stability of the phase angle of the third-order harmonic current for several lamps used [35].

currents for several selected combination types LED-LED and LED-CFL of the lamps used in this work. The corresponding experimental uncertainty (mainly due to statistical fluctuations) was within ±7%.

To find the level of attenuation of the third-order harmonic currents as a consequence of the combinations of lamps, it is useful to define the diversity factor for the harmonic current, as the ratio between the vector sum (as measured) and the arithmetical sum (as calculated) of the third-order harmonic currents:

$$DF_3 \equiv \frac{|\text{vector sum of current harmonic}|}{\text{arithmetic sum of current harmonic}}. \tag{20}$$

Note that a value of $DF_3 \approx 1$ indicates an inadequate combination of lamps, which generates a minimum attenuation of the third-order harmonic currents, whereas $DF_3 << 1$ implies an optimum combination, with a maximum attenuation of this harmonic current. **Figure 9** shows the dependence of measured DF_3 for selected lamp combinations on the difference between the corresponding phase angles of the third-order harmonic currents. The solid curves represent the diversity factor calculated for limit values of the ratio between the amplitudes of the third-order harmonic current of each lamp of the combination (values calculated for a ratio = 1 are indicated with a blue line while for a ratio = 7 with a red line). Note that these values are close to the minimum and maximum ratios obtained in the different combinations proposed, as it was indicated in **Table 4**.

It is seen in **Figure 9** that a number of combinations of LED and CFL lamps lead to a considerably decrease in the content of the third-order harmonic current. As expected, the maximum attenuation of the third harmonic amplitude is achieved with harmonic ratios close to 1 and for harmonic phase angle differences close to 180°. These results are different from those reported by other studies [33, 34] where lower-order harmonics did not exhibit a very large reduction in amplitude. However, it should be noted that in [33, 34] random combinations of lamps were used.

Note that the results presented in **Figure 9** were obtained combining two lamps; however, the same results could be obtained between two arbitrary sets of lamps, provided that each set is formed by the same number of elements. Currently, CFLs are being replaced by LEDs gradually, and in several lighting installations, the two technologies coexist. From the point of view of the reduction of the third harmonic, the combinations of lamps of different technologies are

usually convenient. For the lamps evaluated, the change of technology (CFL to LED) not only improves the level of illumination and reduces the content of third harmonic but also decreases the active power demanded by the installation, reducing also the environmental impact.

In order to better show the contribution of the proposed solution, the measured spectrum of the harmonic currents (expressed in per unit of the fundamental harmonic current), both in

Lamp combination	Ratio between the amplitudes (rms) of the third-order harmonic current of each lamp of the combination
CFL Philips 23 W-LED Philips 18 W	1.1
CFL Philips 15 W-LED Philips 13 W	1.8
LED Lumenac 8 W-LED Sica 9 W	1.9
LED Philips 13 W-LED Sica 13 W	1.9
LED Osram 8 W-LED Lumenac 8 W	2.3
CFL Sica 11 W-LED Philips 9 W	2.6
LED Sica 9 W-LED Philips 9 W	2.8
CFL Sica 11 W-LED Osram 8 W	4.6
CFL Philips 15 W-LED Philips 14 W	4.7
LED Philips 14 W-LED TBC in 14 W 114 W	4.7
CFL Sica 11 W-LED GE 10 W	6.7
CFL Sylvania 20 W-LED Philips 14 W	6.8

Table 4. Tested combinations of lamps [35].

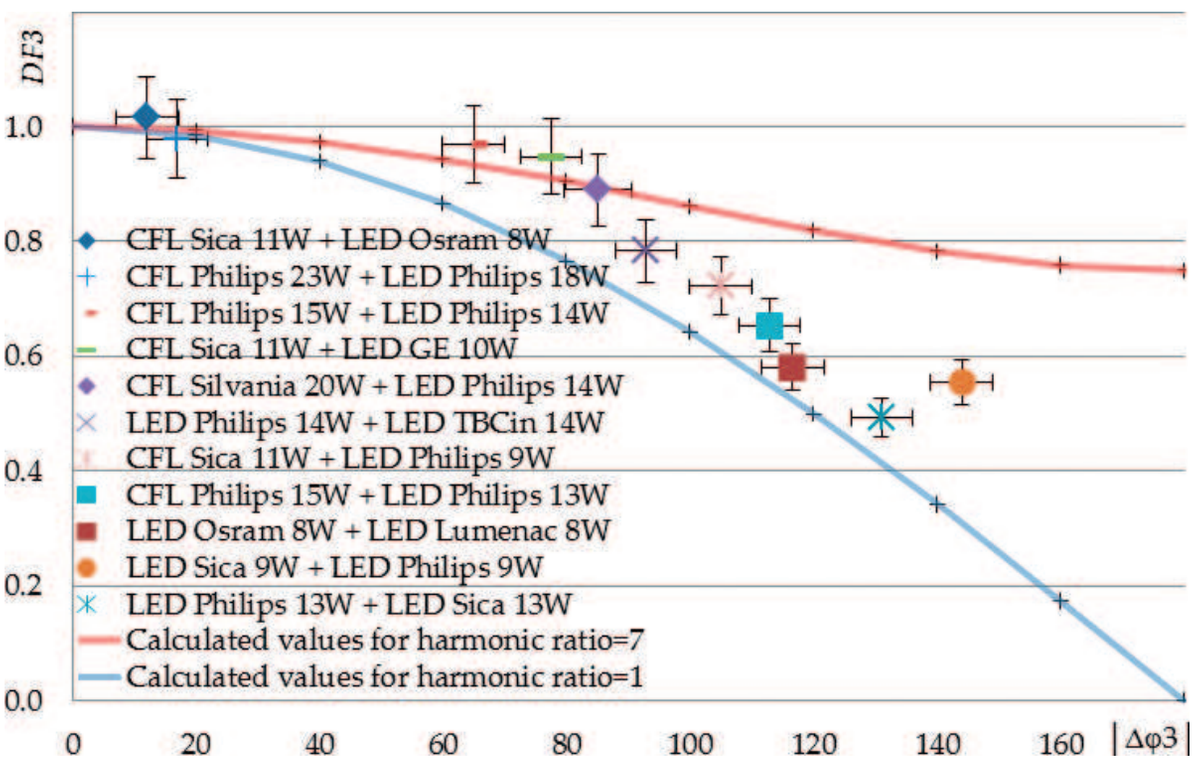

Figure 9. Attenuation of the third harmonic by combination of lamps [35].

http://dx.doi.org/10.5772/intechopen.76752

one phase and in the neutral conductor of a four-core cable, feeding balanced single-phase loads formed by selected LED-LED combination is shown in **Figures 10(a)** and **(b)**, respectively. The corresponding spectrums for the individual lamps are also shown. Harmonic currents up to the order $h = 19$ were measured. In addition, the rms value of the total current in both conductors is presented in **Figures 10(a)** and **(b)**.

It is seen in **Figure 10** that the selected LED combination leads to a significant decrease in the third-order harmonic content of the line current. Notice also that the RMS value of the total current of the combination is considerable lower than the corresponding value of the individual lamp having the higher harmonic content of the combination (LED Sica 9 W), being similar to that of the LED Lumenac 8 W.

As it can be seen in **Figure 10**, the RMS value of the total current of the combination is strongly reduced with respect to that of the LED Sica 9 W, mostly due to a decrease in the content of the third-order harmonic current, although some reduction is also observed for the high-order harmonics. It is important to note that the current of the LED Sica 9 W has a strong component of the third-order harmonic (exceeding the emission limit imposed by IEC as quoted in Section 1) and also of high-order harmonics ($h = 9$ and 15). As the overall harmonic power losses in the neutral conductor depend on the RMS value of the total current, a marked reduction in the harmonic losses with respect to that of the LED Sica 9 W (and even with respect to the LED Lumenac 8 W) is expected for the tested lamp combination.

Notice also the negligible small value of the first-order harmonic current in the neutral conductor due to the balanced loading of the cable. The small residuals observed are due in part to small asymmetries attributable to the constructive differences between the lamps tested.

The cable harmonic power losses can be approximately calculated by Eq. (18). To quantify the reduction in the harmonic power losses due to the lamp combination, it is useful to compare

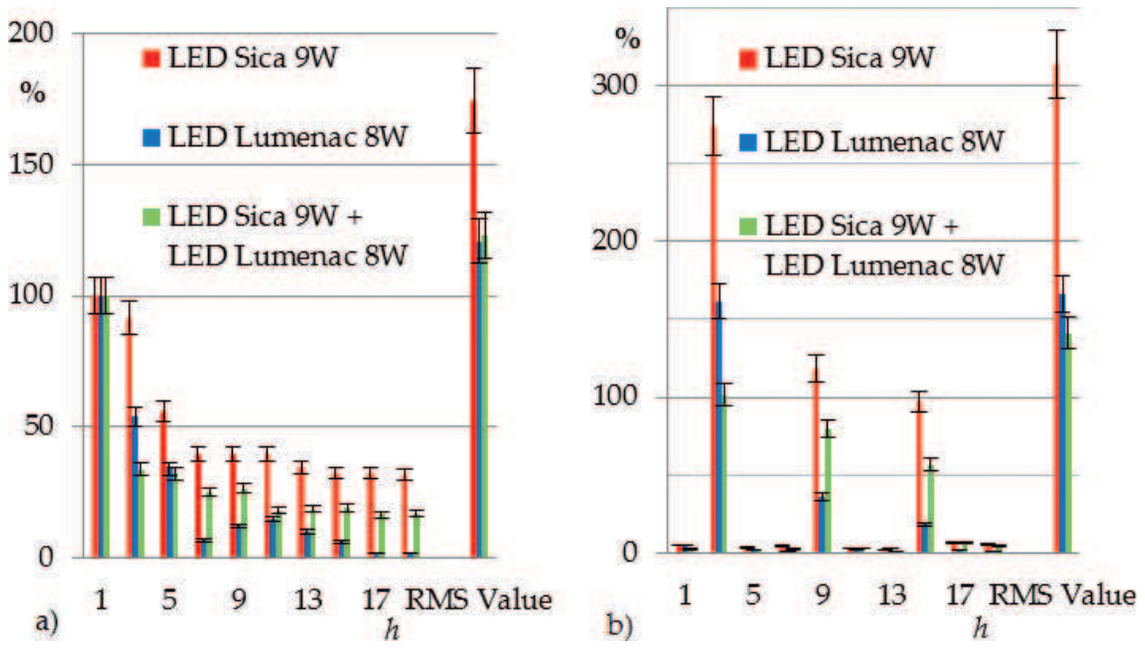

Figure 10. Harmonic current content in one phase (a) and in the neutral conductor (b) of a four-core cable for a selected LED-LED combination.

the above calculated cable losses with the losses produced in an identical cable but carrying an undistorted electric current of the same RMS value as the first harmonic current of the distorted current. To do this, the cable loss ratio defined as

$$\xi \equiv \frac{P_{loss}}{3 {I_{RMS}}^2(1) R_{ac}(1) + {I_{RMS\,N}}^2(1) R_{ac\,N}(1)}, \tag{21}$$

(the first-order harmonic current in the neutral conductor is due to small asymmetries in the single-phase loads) was calculated on the basis of the measured data by neglecting the influence of the harmonic frequency on the resistance of the conductors (i.e. the conductor radius is small compared to the characteristic skin penetration length, and the distances of the nearby conductors are large compared to the conductor radius [29]). For a neutral conductor having a cross section equal to half of the phase conductor section [38], it results in a value of 9.6, 3.3 and 2.8 for the individual lamps LED Sica 9 W and LED Lumenac 8 W and for the combination, respectively, thus showing that the tested lamp combination leads to a significant decrease in the power harmonic losses. A similar result can be obtained for other lamp combination provided that the diversity factor for the third-order harmonic current of the arrangement is small enough.

Note that in lighting loads of substantial power demand such as those considered in this work, it would be convenient from the point of view of the reduction of the power losses to connect the LED lamps between lines (rather than between a line and the neutral conductor). In such case, the third-order harmonic currents (and their multiples) cannot flow through the network since the return path through the neutral conductor does not exist. This suggests the convenience of having LED lamps including ac/dc converters designed to operate as two-phase loads. As quoted before, a large number of the existing low-voltage installations present a neutral conductor with a reduced section (about half of the phase conductor) [38]. These installations when feeding LED loads could present more than twice the losses corresponding to a current without distortion of the same rms as the value of the first harmonic current of the lamps [13]; thus, a marked reduction (over ~ 50%) in the overall harmonic power losses can be expected if the LED lamps (having ac/dc converters designed to operate as two-phase loads) are connected between lines instead as single-phase loads.

4. Conclusions

Calculation of harmonic disturbances in low-voltage network installations having the neutral cross section approximately equal to half of the phase conductors when used for feeding large LED lighting loads was reported. The cables were modeled by using electromagnetic finite element analysis software. Four-core cables and four single-core cable arrangements (three phases and neutral conductor) of small, medium and large conductor cross sections were examined. This study has shown that:

1. The cross section of the neutral conductor plays an important role in the harmonic losses and thus in the derating of the cable ampacity, due to the presence of a high level of triplen harmonics in the distorted current.

2. An incoming widespread use of LED lamps in lighting could create significant additional harmonic losses in the supplying low-voltage lines, and thus more severely harmonic emission limits should be defined for LED lamps.

In order to reduce the third-order harmonic currents in the neutral conductor, an experimental investigation of diversity factors for LED in combination with CFL and LED lamps was also performed. An experimental investigation of diversity factors for LED (light emitting diode) in combination with CFL (compact fluorescent lamps) and LED lamps with nominal powers <25 W was presented. In contrast to other works, attention was paid to the reduction of low-order harmonics, especially the third one, which is mainly responsible for the strong increase in power losses in the neutral conductor of the low-voltage installations. The results showed that a number of selected combinations of LED and CFL lamps lead to a considerable decrease in the content of the third-order harmonic current. These results are different from those reported by other studies where lower-order harmonics did not exhibit a very large reduction in amplitude. However, it should be noted that in those studies random combinations of lamps were used. The convenience of having LED lamps designed to operate as two-phase loads is suggested for certain applications of significant power demand.

Acknowledgements

N. M. and L. P. acknowledge financial support by the National Technological University (PID 3568). L. P. and M. A. L. are members of the CONICET. We have reused our own original work published in *Advanced Electromagnetic Journal* to write part of the presented chapter.

Author details

Natalio Milardovich[1]*, Leandro Prevosto[2], Miguel A. Lara[3] and Diego Milardovich[4]

*Address all correspondence to: njmilardovich@gmail.com

1 Electrical Discharge Group, Department of Electromechanical Engineering, Venado Tuerto Regional Faculty, National Technological University, Venado Tuerto (Santa Fe), Argentina

2 Electrical Discharge Group, Department of Electromechanical Engineering, Venado Tuerto Regional Faculty, National Technological University, CONICET, Venado Tuerto (Santa Fe), Argentina

3 Master in Energy for Sustainable Development, Faculty of Exact Science, Eng. and Surveying, Rosario National University, Rosario (Santa Fe), Argentina

4 Faculty of Exact Science, Eng. and Surveying, Rosario National University, Rosario (Santa Fe), Argentina

References

[1] Subjak JS, Mc Quilkin JS. Harmonics-causes, effects, measurements, and analysis: An update. IEEE Transactions on Industry Applications. 1990;**26**:1034-1042

[2] Wagner VE et al. Effects of harmonics on equipment. IEEE Transactions on Power Delivery. 1993;**8**:672-680

[3] Carpinelli G, Caramia P, Di Vito E, Losi A, Verde P. Probabilistic evaluation of the economical damage due to harmonic losses in industrial energy system. IEEE Transactions on Power Delivery. 1996;**11**:1021-1028

[4] Puchalapalli S, Pindoriya NM. Harmonics assessment for modern domestic and commercial loads: A survey. In: Proceedings of the IEEE International Conference on Emerging Trends in Electrical Electronics & Sustainable Energy Systems (ICETEESES); 11-12 March 2016; India. New York: IEEE; 2016. pp. 120-125

[5] Rice DE. Adjustable speed drive and power rectifier harmonics their effect on power systems components. IEEE Transactions on Industry Applications. 1986;**22**:161-177

[6] Dwyer R, Khan AK, Mc Granaghan M, Tang L, Mc Cluskey RK, Sung R, Houy T. Evaluation of harmonic impacts from compact fluorescent lights on distribution systems. IEEE Transactions on Power Systems. 1995;**10**:1772-1779

[7] Azevedo IL, Morgan MG, Morgan F. The transition to solid-state lighting. Proceedings of the IEEE. 2009;**97**:481-510. DOI: 10.1109/JPROC.2009.2013058

[8] Chong-Tan S. General n-level driving approach for improving electrical-to-optical energy-conversion efficiency of fast-response saturable lighting devices. IEEE Transactions on Industrial Electronics. 2010;**57**:1342-1353

[9] van Driel WD, Fan XJ. Solid state lighting reliability. New York: Springer; 2013. p. 613. DOI: 10.1007/978-1-4614-3067-4

[10] Chen W, Ron Hui SI. Elimination of an electrolytic capacitor in AC/DC light-emitting diode (LED) driver with high input power factor and constant output current. IEEE Transactions on Power Electronics. 2012;**27**:1598-1607

[11] Qu X, Wong SC, Tse CK. Resonance assisted buck converter for offline driving of power LED replacement lamps. IEEE Transactions on Power Electronics. 2011;**26**:532-540

[12] Li S, Tan S-C, Lee CK, Waffenschmidt E, Ron Hui SI, Tse CK. A survey, classification, and critical review of light-emitting diode drivers. IEEE Transactions on Power Electronics. 2016;**31**:1503-1516. DOI: 10.1109/TPEL.2015.2417563

[13] Milardovich N, Prevosto L, Lara MA. Calculation of harmonic losses and ampacity in low-voltage power cables when used for feeding large LED lighting loads. Advanced Electromagnetism. 2014;**3**:50-56. DOI: 10.7716/aem.v3i1.258

[14] Gu L, Ruan X, Xu M, Yao K. Means of eliminating electrolytic capacitor in AC/DC power supplies for LED lightings. IEEE Transactions on Power Electronics. 2009;**24**:1399-1408

[15] Ruan X, Wang B, Yao K, Wang S. Optimum injected current harmonics to minimize peak-to-average ratio of LED current for electrolytic capacitor-less AC-DC drivers. IEEE Transactions on Power Electronics. 2011;**26**:1820-1825

[16] Arias M, Lamar DG, Sebastian J, Balocco D, Diallo AA. High-efficiency LED driver without electrolytic capacitor for street lighting. IEEE Transactions on Industry Applications. 2013;**49**:127-137

[17] Lo YK, Wu KH, Pai KJ, Chiu HJ. Design and implementation of RGC LED drivers for LCD backlight modules. IEEE Transactions on Industrial Electronics. 2009;**56**:4862-4871

[18] Muthu S, Schuunnans FJ, Pashley M. Red, green, and blue LEDs for white light illumination. IEEE Journal of Quantum Electronics. 2002;**8**:333-338

[19] Hui SYR, Qin YX. A general photoelectro-thermal theory for light emitting diode (LED) systems. IEEE Transactions on Power Electronics. 2009;**24**:1967-1976

[20] Chen HT, Tan SC, Hui SYR. Color variation reduction of GaN-based white light emitting diodes via peak-wavelength stabilization. IEEE Transactions on Power Electronics. 2014; **29**:3709-3719

[21] Uddin S, Shareef H, Mohamed A, Hannan MA. An analysis of harmonics from LED lamps. In: Proceedings of the Asia-Pacific Symposium on Electromagnetic compatibility (APEMC); 21-24 May 2012; Singapore. New York: IEEE; 2012. pp. 837-840

[22] Uddin S, Shareef H, Mohamed A. Power quality performance of energy-efficient low-wattage LED lamps. Measurement. 2013;**46**:3783-3795

[23] Castro AG, Rönnbergb SK, Bollen MHJ. Light intensity variation (flicker) and harmonic emission related to LED lamps. Electric Power Systems Research. 2017;**146**:107-114

[24] Aman MM, Jasmon GB, Mokhlis H, Bakar AHA. Analysis of the performance of domestic lighting lamps. Energy Policy. 2013;**52**:482-500

[25] Desmet JJM, Sweertvaegher I, Vanalme G, Stockman K, Belmans RJM. Analysis of the neutral conductor current in a three-phase supplied network with nonlinear single-phase loads. IEEE Transactions on Industry Applications. 2003;**39**:587-593

[26] Meliopoulos APS, Martin MA Jr. Calculation of secondary cable losses and Ampacity in the presence of harmonics. IEEE Transactions on Power Delivery. 1992;**7**:451-459

[27] Demoulias C, Labridis DP, Dokopoulos PS, Gouramanis K. Ampacity of low-voltage power cables under nonsinusoidal currents. IEEE Transactions on Power Delivery. 2007; **22**:584-594

[28] Hiranandani A. Calculation of cable ampacities including the effects of harmonics. IEEE Transactions on Industry Applications. 1998;**4**:42-51

[29] Chien CH, Bucknall RWG. Harmonic calculations of proximity effect on impedance characteristics in subsea power transmission cables. IEEE Transactions on Power Delivery. 2009;**24**:2150-2158

[30] Emanuel AE, Yang M. On the harmonic compensation in nonsinusoidal systems. IEEE Transactions on Power Delivery. 1993;**8**:393-399

[31] Lai JS, Key TS. Effectiveness of harmonic mitigation equipment for commercial office buildings. IEEE Transactions on Industry Applications. 1997;**33**:1104-1110

[32] Chitra R, Neelaveni R. A realistic approach for reduction of energy losses in low voltage distribution network. International Journal of Electrical Power & Energy Systems. 2011;**33**: 377-384

[33] Uddin S, Shareef H, Mohamed A, Hannan MA. An analysis of harmonic diversity factors applied to LED lamps. In: Proceedings of the IEEE International Conference on Power System Technology (POWERCON); 30 Oct-2 Nov 2012; New Zealand. New York: IEEE; 2012. pp. 1-5

[34] Cuk V, Cobben JFG, Kling WL, Timens RB. An analysis of diversity factors applied to harmonic emission limits for energy saving lamps. In: Proceedings of the IEEE International Conference on Harmonics and Quality of Power (ICHQP); 26-29 Sept 2010; Italy. New York: IEEE; 2010. pp. 1-6

[35] Milardovich N, Prevosto L, Lara MA, Milardovich D. On the reduction of the third-order harmonic losses in low–voltage power cables used for feeding large LED and CFL lighting loads. Advanced Electromagnetism. 2017;**6**:46-52. DOI: 10.7716/aem.v6i3.542

[36] Limits for harmonic current emissions (equipment input < 16A per phase), IEC 61000-3-2: 2014

[37] Cables for rated voltages of 1 kV, IEC 60502-1: 2004 (E)

[38] Distribution cables of rated voltage 0.6/1 kV, CENELEC Std. HD603 S1:1994/A2: 2003 E

[39] QuickField Lite, which is a commercially available electromagnetic finite-element analysis software manufactured by Tera Analysis Ltd. QuickField Lite [Internet]. 2017. Available from: https://quickfield.com/edu_lic.htm [Accessed: January 12, 2017]

[40] International standard of resistance for copper, IEC 60028 Ed. 2.0 B: 1925

[41] Electrical Installations of Buildings—Part 5: Selection and Election of Electrical Equipment—Section 523: Current-Carrying Capacities in Wiring Systems, CENELEC Std. HD384.5.523, 2001, S2. Iec 60287

[42] Electric cables-Calculation of the current rating, IEC 60287-1-1, CEI/IEC 60287-1-1:2006